Hybrid-electric power unit for an ultralight aircraft

A. M. Pisapia[1], A. Volza[1], T. Savioli[2], P. Martini[3], E. Mattarelli[1,a]

[1] Dipartimento di Ingegneria “Enzo Ferrari”, Università di Modena e Reggio Emilia, via Pietro Vivarelli 10, 41125 Modena

[2] Atris Engineering s.r.l., via Ettore Orlandi 8, 41122 Modena

[3] Studio tecnico agrario, via Carlo Cattaneo 48, 41126 Modena

[a] Corresponding author: enrico.mattarelli@unimore.it

High power-weight ratio, reliability and efficiency are the main design goals for the propulsion system of ultralight aircraft (mass up to 650 kg). For power outputs beyond 40 kW, 4-stroke multi-cylinder SI engines are the most widespread solution, while pure electric powertrains do not appear at the moment as a practical proposition. Four stroke diesel engines would also be very attractive, in particular for military applications, but their weight is significantly higher than their gasoline powered counterpart.
The goal of the study presented in this article is to develop a hybrid-electric power unit for ultralights, running on heavy fuels (diesel, kerosene, jet fuels). Reference is made to Falco EVO, by Leonardo, originally equipped by the Rotax 912 ULS/S engine (peak power 73.5 kW, weight about 60 kg): the proposed power unit has the same cylinders layout, smaller overall dimensions and almost equivalent weight. The thermal engine is an innovative two-stroke unit, coupled in parallel to a permanent magnet electric motor. The design and optimization of the hybrid power unit has been supported by CAE tools, including CAD and CFD simulations.
The results of the study show that the new hybrid system can save about 30% of fuel mass at the typical cruise conditions, and it can increase the peak power output up to 20%, compared to the reference Rotax engine. The reduction of fuel consumption can be translated into an equivalent increment of the operative range of the aircraft, or into an increase of payload (+30%, considering the Falco EVO aircraft). Finally, compared to the Rotax engine, the hybrid power unit exhibits significantly lower CO2 emissions (from -12% to -37%), thanks to the improvement of fuel efficiency.

Keywords: two stroke engine, electrification, power unit, ultra-light aircrafts, 1D CFD, CAD for design

Nomenclature	
4S	4-Stroke
2S	2-Stroke
ICE	Internal Combustion Engine
SI	Spark Ignition
CI	Compression Ignition
EM	Electric Motor
NMC	Nickel Manganese Cobalt
HPU	Hybrid Power Unit
EMG	Electric Motor Gearbox
PG	Propeller Gearbox
HL	Hybridization Level
BP_A	Battery Pack A (small)
BP_B	Battery Pack B (big)
IMEP	Indicated Mean Effective Pressure
BMEP	Brake Mean Effective Pressure
BSFC	Brake Specific Fuel Consumption
SL	Sea Level

INTRODUCTION

According to market data, the ultra-light aircraft sector is growing at a fast pace: forecasts indicate a $2.61 billion increase in the period 2022-2026 and a 5.71% compound annual growth rate in the following years [1]. In addition to the military sector, the interest towards ultralights extends also to the fields of civil transport, leisure and sport. This trend will lead to an increasing demand of propulsion systems, encouraging the development of alternative power units. For power outputs above 40 kW, 4-Stroke (4S) Spark-Ignition (SI) engines are the most widespread solution. The Rotax 912 ULS/S (73 kW [2]), Jabiru 2200 (60 kW [3]) and HKS 700e (44 kW [4]) are probably the best known engines in this category. The 74 kW Danielson 4S engine [5] is different, as it adopts compression ignition (CI) and runs on diesel, kerosene or heavy fuels, instead of Avio gasoline. Except the Danielson, all the above mentioned engines are naturally aspirated, and have a weight of about 50-70 kg.

Electric propulsion would provide undisputable advantages: no exhaust emissions, possibility to have high power outputs for a limited amount of time, silent operations, low thermal trace. On the other hand, a full electric propulsion system does not appear as a practical proposition, since the weight of the battery would strongly limit the range of the aircraft. As an example, a take-off of 5 minutes with a power of 72 kW at the propeller, would require an energy stored in the battery of about 7.5 kWh, assuming an efficiency of the electric propulsion system equal to 80% (product of the efficiencies of battery, inverter and electric motor). Therefore, supposing a minimum state of charge of 0.2, the battery should have a capacity of 7.5/0.8=9.4 kWh. Even adopting the best technology currently available for maximizing the energy density stored in the battery (≈0.2 kWh/kg, with Li-Po cells), and disregarding the problem of the maximum discharge rate of the battery, the weight of the pack would be close to 50 kg, just for supporting the take-off phase.

Hybrid powertrains, coupling the internal combustion engine (ICE) to an electric motor (EM), appears as a more viable solution to merge the advantages of both propulsion systems, mitigating their drawbacks. However, if the combustion engine is developed with a standard technology, the increase of weight is unavoidable. It is worth noting that this aspect is much more important for aircraft, compared to road vehicles.

A significant reduction of the thermal unit weight can be obtained passing from the 4S to the 2S cycle [6]. Unfortunately, for power above 40 kW, the standard 2S design with piston controlled ports and cranckcase pump is typically affected by high fuel consumption and poor reliability [7]. A more robust and efficient 2S design can be found in the WAM engine [8], [9], but its weight is significantly higher than the Rotax 912.
The goal of this study is to demostrate the potential of a Hybrid Power Unit (HPU) which combines the advantages of a new type of 2S engine with those of electric motors.
The thermal unit of the proposed HPU consists of a four-cylinder boxer air-cooled 2S compression ignition engine, running on diesel (or kerosene and jet fuels, with minor modifications). The electric motor is a commercial axial flux unit (Emrax 188), connected in parallel to the thermal engine, as it will be shown in the next section. The ICE can be disengaged by a clutch, permitting a full electric operating mode. Moreover, the ICE can charge the battery, whenever the torque required by the propeller is lower than the maximum load of the thermal engine.
While hybrid power units are a standard technology in the automotive sector, they still represent a novelty in the aviation field. From a theoretical point of view, HPU for light aircraft have been already investigated [10]–[13] but at the time of writing this paper, no prototype has reached the market.
The main novelty of this study is the design of the 2S engine, featuring an original combustion system, based on a commercial high pressure injection system, originally developed for gasoline engines. Despite the relatively low injection pressure (50-350 bar), the proposed 2S engine can burn diesel and heavy fuels in a very efficient way, as demonstrated by specific CFD-3D simulations (not shown in the article, for confidentiality reasons). In comparison to a conventional Common Rail, the adopted injection system is considerably lighter and more compact.
In order to put the project into a context, reference is made to the worldwide bestseller 4S engine for ultralights, the Rotax 912 ULS/S.
The results presented in the study show that the proposed HPU can provide at least the same performance of the Rotax 912 ULS/S, with a minimum increase of weight. The advantages expected by the new powerunit, in comparison to the reference engine, are summarized below.

- Noticeable reduction of fuel consumption, and, consequently, of CO2 emissions;
- higher fuel flexibility: almost all types of fuels for compression ignition engines can be used (diesel, kerosene, heavy fuels..)
- longer aircraft range, for the same mass of fuel, or higher payload for the same range
- Higher power output, even if for a limited amount of time
- Full electric mode, for a limited amount of time
- High electric power available for specific devices installed on the aircraft
- Lower risk of fire (diesel fuel is less dangerous than gasoline)

The authors ackowledge that the current study is just a first step for the development of a novel HPU: more accurate analyses will follow, possibly with the support of experimental data.

POWERUNIT LAYOUT

The hybrid propulsion system, shown in figure 1, is of the parallel type, a quite common choice for light aircraft, as it maximizes the peak power (a very useful capability during take-off or emergency manoeuvres) and it increases the average ICE thermal efficiency at cruise conditions, when load is typically low (thanks to the assistance of the EM, an ICE of smaller capacity can be selected) [12].

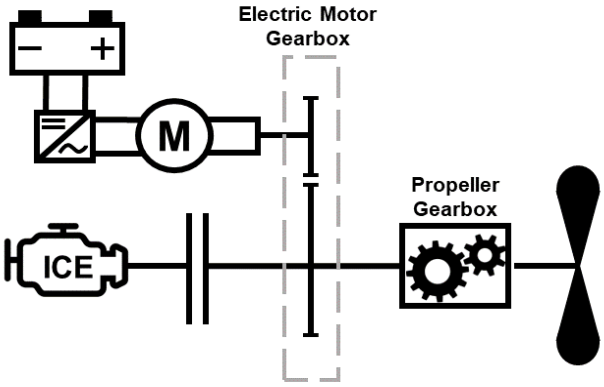

Figure 1. Sketch of the HPU layout.

The thermal engine, described in the following section, is connected to the propeller via a dry slip clutch, which enables a smooth transmission of the instantaneous torque even without a flywheel, saving some weight.
The EM is the Emrax 188, a light and compact axial flux permanent magnet machine (it weighs 7.5 kg, for a maximum continuous power of 35 kW; the external diameter of the rotor is 188 mm). The component is connected to the propeller through the Electric Motor Gearbox (EMG), a couple of gears, with a ratio equal to 0.75.
The Propeller Gearbox (PG), between the hybrid power unit and the propeller, is designed in order to get a maximum propeller speed equal to that of a commercial unmanned aircraft (Falco EVO [14]), powered by the Rotax 912 ULS/S engine. The purpose of this choice is to permit a straightforward comparison between the proposed configuration and a conventional one, selected among the most widespread in the market.
The battery is made up of cylindrical lithium cells that use the NMC technology, which has been chosen for its high specific power [15]. As far as the battery capacity is concerned, two options are studied, referred to as BP_A (the smaller) and BP_B (the bigger). Besides weight and energy storage, the battery size affects also the maximum power generated by the power unit and its maximum hybridization level. Hybridization Level (HL) is defined as the ratio between the power delivered by the battery and the power provided by the thermal engine.

$$HL = \frac{P_{batt}}{P_{eng}} \quad (1)$$

HL depends on the control strategy of the power unit. Table 1 reviews the characteristic of the two battery packs, showing also the values of HL at take-off and at peak power. Concerning the take-off phase, we assumed a power rate corresponding to the peak delivered by the Rotax 912 ULS/S engine. During this manoeuvre, the electric motor must provide a power of 5 kW to compensate the lower maximum output of the 2S engine. Conversely, at peak power condition the limit of EM is related to the discharge capabilities of the battery.
As expected, BP_B allows the system to achieve higher performance and higher levels of hybridization, but it is slightly heavier. The choice between the two packs depends on the specific project targets of the aircraft. A high HL would be particularly useful to support the thermal engine at high altitudes, where the air density drops, along with the ICE performance outputs. In these conditions, only a slight penalization on the cooling of the electric components is expected.
The analysed propulsion system can operate in four modes:

- Internal Combustion Engine (ICE) only
- Electric motor (EM) only

- ICE+EM in parallel
- ICE and electric power generator for propulsion and battery charging

Obviously, the proposed power unit is a mild hybrid, as electric propulsion can be used for a limited amount of time during the mission. A full hybrid configuration was discarded because of the weight constraints for this class of aircraft.

Table 1. Main characteristics of the battery packs.

	Cell layout	Rated Capacity	Nominal Voltage	Max. continuous discharge power	Max. continuous discharge power with 80°C cut temperature	Cells weight	Battery pack weight	Take-off phase HL	Max HL
		[kWh]	[V]	[kW]	[kW]	[kg]	[kg]	[\]	[\]
BP_A	S34P3	1.43	122.4	12.9	16.5	7.1	7.9	0.14	0.25
BP_B	S34P5	2.39	122.4	21.4	27.5	11.9	13.1	0.14	0.41

DESIGN OF THE 2-STROKE ENGINE

The cylinder geometry of the proposed 2-stroke engine is designed according to the concepts described in some previous technical papers, in particular in [10]: the inlet and exhaust ports are controlled by the motion of the piston, while air is pumped into the cylinder via a mechanical supercharger. The adoption of an external scavenge pump permits the implementation of a lubrication system identical to a 4S engine; therefore, the fresh charge enters the cylinder directly, and it does not contain neither lubricant nor fuel (the latter is injected after the closure of all the cylinder ports). Without the connection to the crankcase, the design of the inlet ports can be optimized in a quite free manner, compared to a conventional crankcase scavenged 2-stroke engine.

The most critical aspect of the cylinder design is the combustion system. Due to the particular type of turbulence within the cylinder (a strong tumble vortex, generated by the flux of fresh charge directed along the liner and deviated by the cylinder head), it is not convenient to implement a conventional system, made up of an omega-shaped bowl in the piston and a flat cylinder head. In fact, this design requires a well-structured swirl motion, that cannot be created without spoiling the efficiency of the loop scavenging process. On the other hand, the absence of valves makes the design of the cylinder head and of the piston crown almost completely free of constraints. This freedom has been exploited for the implementation of a novel combustion system, characterized by a very high compression ratio (>22) and a compact chamber (low surface-to-volume ratio). Several CFD simulations carried out by the authors revealed that this combustion system can burn diesel fuel quite efficiently, even with very low injection pressures, compared to standard CI engines. The simulations were conducted at engine speeds up to 5000 rpm, with values of relative air-fuel ratio higher or equal to 1.3, and for IMEP up to 10 bar (beyond the last limit, combustion tends to become rough, due to the increase of the maximum rate of pressure rise). As an example, Figure 2 shows the pressure trace within the cylinder and the burnt fraction, calculated for an optimized injection strategy, at 5000 rpm, IMEP=10.3 bar.

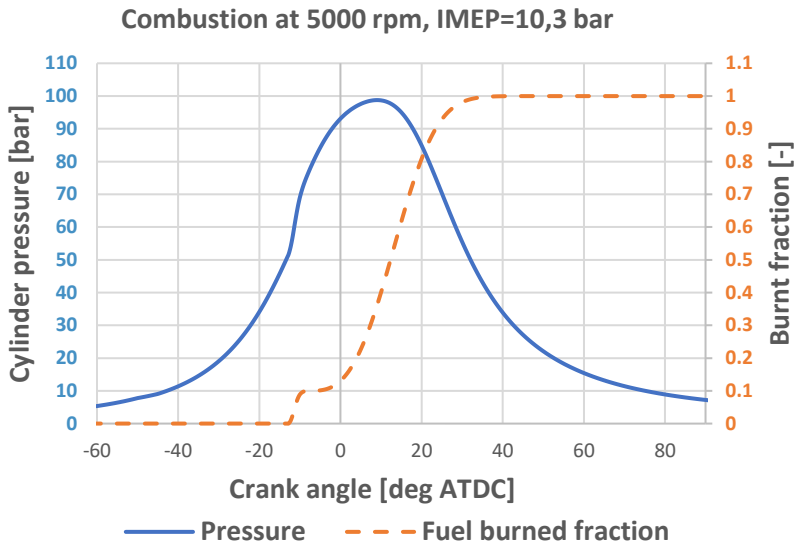

Figure 2. Combustion characteristics at 5000 rpm, IMEP=10.3 for an optimized injection strategy.

At the moment of writing this paper, the details of the combustion system are still confidential and they cannot be disclosed here. However, in the next section, the other criteria followed for the development of the engine are presented.

For the selection of the total displacement, we considered, as a first attempt, a target power of 70 kW at 5000 rpm, with a corresponding BMEP of 8 bar. It should be noted that the low value of BMEP helps the designer to limit the combustion roughness, and, in general, to maintain high level of mechanical reliability even in presence of a lightweight construction. In addition, the relatively low amount of rejected heat enables the adoption of an air cooling system, with ensuing advantages in terms of weight, compared to a more conventional liquid cooling.

From the hypotheses reported above, the resulting engine capacity is 1050 cc. The number of cylinders is set at 4, as on most ultralight aircraft engines, included the reference Rotax 912 ULS/S. Also, the cylinders layout (boxer) is identical, in order to get a smooth instantaneous torque output, a fundamental aspect to reduce the mechanical stress of the propeller.

The bore-to-stroke (B/S) ratio is chosen on the basis of the following considerations:

- B/S<1 helps to reduce the work required to pump air into the cylinders;
- Long strokes generate high mean piston speeds, with an ensuing increase of mechanical friction losses and of inertia forces

Assuming a maximum mean piston speed of 13.5 m/s at 5000 rpm, a typical limit for automotive 4S diesel engines, the corresponding maximum length of the stroke would be 81 mm. The bore value corresponding to that stroke and to the cylinder unit displacement (1050/4=262.5 cc) would be 64.2 mm (B/S=0.79). After some iterations, the value of bore and stroke was set at 65 and 79.5 mm, respectively, with B/S=0.82. The final total displacement of the engine is 1055 cc.

In the choice of the air feed system, turbocharging was discarded because a 2S engine without crankcase pump needs a mechanical supercharger to be started. A 2-stage supercharging system, as described in [16], [17], is out of question, because of its weight.

The choice of the mechanical supercharger has been driven by the calculation of the maximum airflow rate required by the engine at maximum power (70 kW@5000 rpm). At this condition, a value of brake specific fuel consumption equal to 240 g/kWh was assumed, on the basis of some preliminary CFD-1D and 3D simulations. The resulting mass flow rate of fuel is: 240 [g/kWh] x 70 [kW] /1000 = 16.8 kg/h. The CFD simulations performed to support the development of the combustion system revealed that the ratio of trapped air to fuel should be at least 20, in order to guarantee a complete and efficient combustion. Therefore, considering a trapping efficiency (air trapped within the cylinder divided by the

air delivered to the cylinder) equal to 80%, on the basis of previous simulations, the airflow rate required by the 2-S engine at maximum power can be estimated as: 16.8 [kg/h] x 20 / 0.8 = 420 kg/h =0.117 kg/s. It should be observed that the corresponding volumetric efficiency (or delivery ratio, according to the nomenclature followed in 2-S engine design), assuming an air density in the ambient of 1.2 kg/m^3, is slightly higher than 1. More precisely, delivery ratio = 0.117 [kg/s] /1.2 [kg/m^3] / 1.055 [L] /5000 [rpm] x 60000 = 1.11. This outcome means that the conditions at which the scavenge process occurs in the proposed 2-stroke engine are quite similar to the ones that may be found in a conventional crankcase scavenged engine, with a tuned exhaust system. As a result, most of the well-established design criteria adopted for conventional 2-S engines can be imported also in this project. This aspect is of fundamental importance, in order to limit the number of parameters that are to be optimized with the support of CFD simulation (see next section).
Two options are available for the choice of the mechanical supercharger: a positive displacement machine, or a centrifugal compressor. According to our simulations, performances are quite similar; however, the centrifugal compressor was preferred for its lower weight.
The development and optimization of the 2-stroke engine, mainly driven by CFD-1D simulations, is discussed in a next section. The final design characteristics of the optimized engine are summarized in table 2.

Table 2. Main design characteristics of the optimized 2S CI engine.

Parameter	Value
Displacement	1055 cc
Number of cylinders, layout	4, boxer
Stroke	79.5 mm
Bore	65 mm
Bore-to-Stroke ratio	0.82
Compression ratio	24
Scavenging Type	Loop, valveless
Scavenge ports advance/delay from BDC	53/53 CA
Exhaust ports advance/delay from BDC	72/72 CA
Supercharging system	Mechanical centrifugal compressor
Max. corrected mass flow rate of the supercharger	0.275 kg/s
Fuel	Kerosene, diesel, jet fuel (JP8)
Max. Injection Pressure	350 bar
Lubrification System	Dry Sump
RPM range	2000-5000 rpm

WEIGHT AND DIMENSIONS

In order to avoid any impact on aerodynamics, the new power unit must be able to replace the stock engine without any significant modification to the fuselage, as well as to the aircraft weight distribution: therefore, the HPU overall dimensions should be smaller or equal than the original equipment, and weighting about the same. Moreover, also the heat exchangers must have the same size: therefore, the total heat rejected by the new HPU should be lower or equal.
It should be noted that also the thermal efficiency of the internal combustion engine has a fundamental influence on an ultralight aircraft total weight: for a given mission range, the lower the fuel consumption, the lighter the fuel tank and the higher the payload.

All the components of the proposed 2-Stroke engine have been designed according to the standard engineering practice, integrated by some empirical hypotheses, based on the authors' experience. In detail, table 3 presents the safety coefficients for the three main components of the crank mechanism: piston, pin, connecting rod and crankshaft.

Table 3. Crankshaft components safety coefficients.

Component	**Section/ Safety coefficient**
Pin	Maximum shear stress section (shear stress)/ 1.46
Connecting rod	Minimum connecting rod section (normal stress)/ 1.46
Connecting rod	Journal cross section (bending-torsion stress)/ 1.42

Table 4. detailed table of components weights

Group level 0	**Group level 1**	**Group level 2**	**Mass [kg]**	**Units [-]**	**Components mass [kg]**	**Subsystem mass [kg]**
Thermal engine	Crankshaft	Piston & Pin	0.41	4	1.64	38.9
		Conn. Rod	0.41	4	1.64	
		Shaft & Bearings	8.25	1	8.25	
	Engine case	Cylinder block	7.72	2	15.43	
		Head	1.06	4	4.24	
	Supercharging system	Compressor & gears	5.10	1	5.10	
	Injection system	Injector & Rail	0.4	4	1.60	
		HP Pump	1.00	1	1.00	
Electric System	Electric motor	Electric motor	7.50	1	7.50	22.9 (28.2)
	Inverter	inverter	2.7	1	2.7	
	1.4 (2.4) kWh battery	Battery & BMS & Case	7.88 (13.14)	1	7.88 (13.14)	
	Electrical wiring	Electrical wiring	4.86	1	4.86	
Configuration						Total mass [kg]
HPU 1.4 kWh battery configuration						61.8
HPU 2.4 kWh battery configuration						67.1

Once all the engine parts were defined, including the materials and the construction technology, the weight assessment was performed using a student edition CAD (Parametric Creo). The same tool was used to draw from scratch a 3D model of the engine assembly, from which it was possible to estimate the overall dimensions of the thermal unit. Figure 3 shows the proposed engine, providing information on its dimensions while table 4 gives detailed information on weights of the 2S engine components. All the dimensions of the new thermal unit are considerably smaller than those of the reference Rotax 912 ULS/S engine [2], leaving plenty of space in the fuselage for the installation of the electrical parts (electric motor, battery, inverter, wirings).

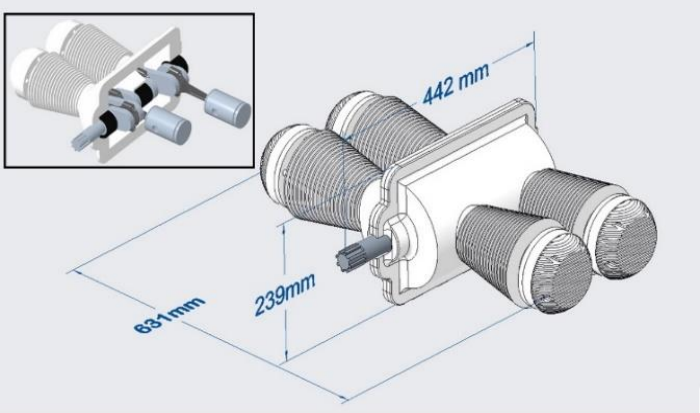

Figure 3. 2S Engine perspective view and size information

While Rotax 912 ULS/S weights 60 kg, the new HPU weights 61.8 kg or 67.1 kg, depending on which battery is considered (BP_A or BP_B). As it will be shown in the next section, the additional weight is compensated by a much better fuel economy.

In both battery configurations, the new HPU holds significant market competitiveness, in terms of power-to-weight ratio. Figure 4 shows power-to-weight ratio in four different cases: the 2S engine alone, the two HPU configurations with different battery capacity, and the Rotax 912 ULS/S engine. In the configuration without considering the fuel tank (referred to as "W/O_Tank") , the advantage of HPU is quite limited. The true strength of the HPUs emerges when considering the presence of a fuel tank with a capacity of 100 liters (referred to as "W_Tank", in figure 4). Assuming that, on average, the HPU fuel consumption is 30% lower than the Rotax 912 ULS/S engine, the weight of the fuel for the same mission passes from 77 kg of gasoline to 54 kg of diesel. The HPUs with fuel tank show higher power-to-weight ratios compared to the Rotax engine, with a 31% increase for the 1.4 kWh battery configuration and a remarkable 38% increase for 2.4 kWh battery configuration.

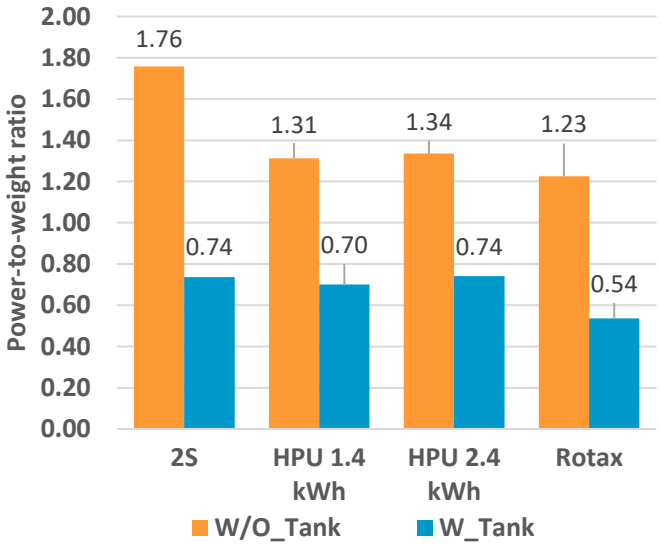

Figure 4. Power-to-weight ratio of different power units, with and without tank (W_Tank, W/O_Tank)

Figure 4 also shows that the 2S engine alone has a better power-to-weight ratio than the Rotax (+40%, curb weight), but at the moment it is not able to provide the same power output.

CFD ANALYSES AND OPTIMIZATION RESULTS

CFD simulation is in general a very important tool to support the development of a new engine, but, without any direct experimental reference, it becomes essential. The numerical approach followed in this study is presented in many other papers ([10], [18]–[24]), and nowadays it can be considered as a standard engineering practice. Since it has not yet been possible to validate the numerical models with experimental data, the authors acknowledge that the results of the study may be affected by some uncertainties. However, all the numerical models employed in the study are derived, more or less closely, from similar previous projects where experimental data were used to calibrate and validate the simulation. In particular, reference was made to the study reported in [10], for the modelling of the flow through the cylinders and for the supercharging system (the geometry of the cylinder ports is the same, as well as the supercharger). It should be also noted that all the technologies employed in the design of the proposed engine are well known, and they do not require any specific approach for their modelling. The optimization process, driven by CFD-1D simulations with GT-Power (Gamma Technologies), started after the definition of the cylinder geometry, based on several CFD-3D analyses, not reported in the current paper, for the sake of brevity.

The goal of the CFD-1D optimization is to find the best trade-off between maximum power and brake thermal efficiency at high speed. Ambient conditions are set considering the International Standard Atmosphere (15 °C for air temperature and 1.013 bar for pressure). A peak cylinder pressure of 100 bar was assumed as a maximum limit, while for the choice of the maximum engine speed, a minimum brake power output of 65 kW was imposed. The most important parameters which have been optimized are listed below.

- Timing (height) of the scavenge (inlet) and exhaust ports
- Transmission ratio between engine and supercharger
- Layout and dimensions of the exhaust system, including the silencer (inlet/outlet diameter and length of each pipe, volume of the junctions and of the chambers of the silencer, ..)
- Dimensions of the intake manifold, between the supercharger and the cylinders

Obviously, each parameter has an influence on the others, so that an iterative process was followed, with the support of Design of Experiments (DoE). Figure 5 provides an overview of the optimization process flow. 1D CFD simulation results are shown in figure 6-11.

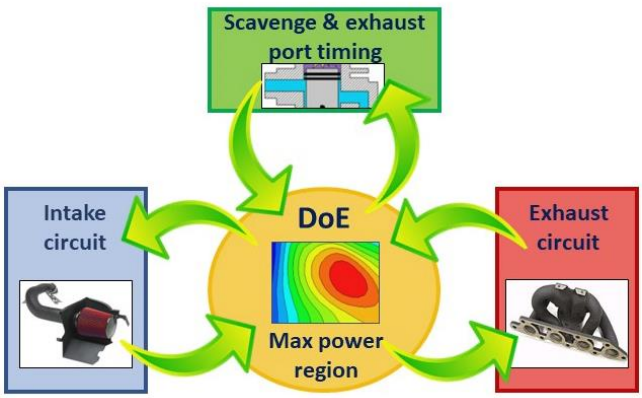

Figure 5. CFD-1D Optimization process

Figure 6a shows a map of Brake Specific Fuel Consumption (BSFC) calculated as a function of engine speed and brake power. Two fundamental sets of data are also shown in the map:

1. Engine full load curve
2. Propeller load curve

The former obviously represents the maximum brake output of the proposed 2S engine as a function of engine speed, after the numerical optimization and considering all the design constraints. The latter is the power required at each speed by the propeller of the FALCO-EVO aircraft, when equipped by the Rotax 912 ULS/S engine (we suppose to use the same propeller also for the hybrid power unit). The region of highest interest in the map, for an aircraft application, is the area between the two curves.
Figure 6a suggests the considerations exposed in the following.

- The 2S engine is able to match the propeller load up to 4230 rpm (58 kW); over this speed, it needs a small support from the EM (5 kW at maximum, in order to reach the output of 73.5 kW provided by the Rotax engine during take-off)
- The typical values of BSFC in the region of interest are between 230 and 240 g/kWh; the best and the worst value is 220 and 265 g/kWh, respectively.

The good fuel efficiency of the new engine is demonstrated by the comparison with the Rotax, shown in table 5, considering the propeller load curve.
Figure 6b shows a map of BMEP as a function of engine speed and brake power: it is observed that the region of interest, between the maximum engine load and the propeller load, is characterized by low values of BMEP (2-8.7 bar). This aspect is very positive, as low values of BMEPs generally correspond to a low level of thermal stress on the cylinder components. Moreover, for the proposed 2S engine there is no need to distinguish between take-off and continuous operating conditions

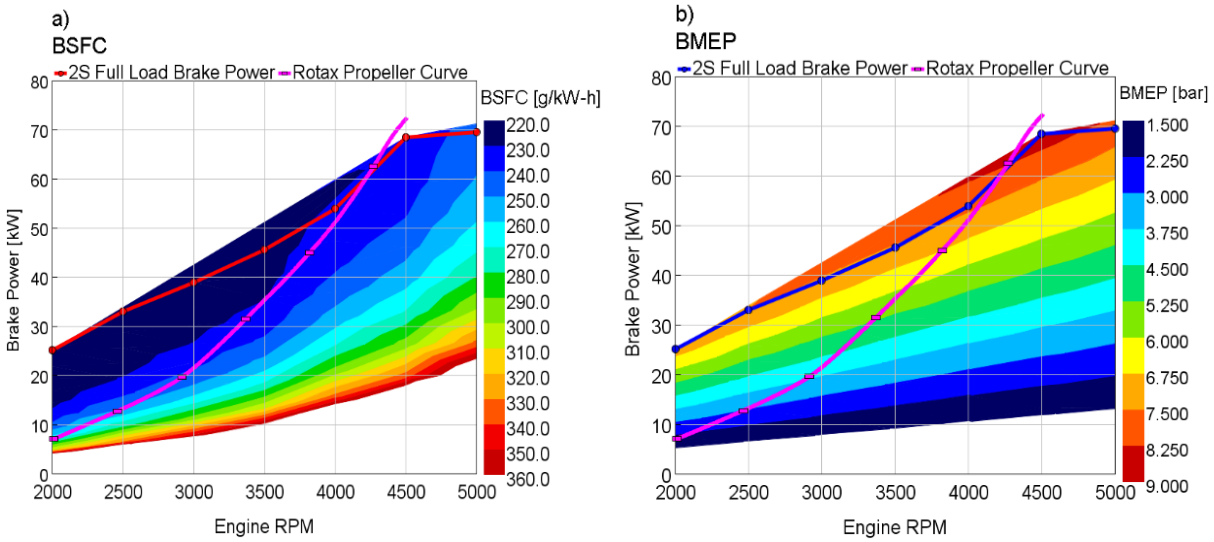

Figure 6a. BSFC map including engine max power curve and propeller resistance curve
Figure 6b. BMEP map including engine max power curve and propeller resistance curve

Table 5. table of fuel consumption on propeller curve

% of max propeller power	Rotax 912 ULS/S speed	2S speed	Propeller power	Rotax 912 ULS/S power	2S power	Rotax 912 ULS/S BSFC	2S BSFC
[%]	[rpm]	[rpm]	[kW]	[kW]	[kW]	[g/kWh]	[g/kWh]
100	5800	4500	73.5	73.5	68.4	282.3	232
90	5600	4350	66.1	66.1	64.0	305	232
75	5270	4100	55.1	55.1	55.1	321	233
60	4880	3790	44.1	44.1	44.1	331	233
50	4560	3550	36.7	36.7	36.7	344	233
40	4240	3300	29.4	29.4	29.4	364	235

Since an aircraft engine must operate at different altitudes, simulations were performed to predict the influence of this parameter. The ambient conditions correspond to the International Standard Atmosphere (ISA), conventionally adopted for the assessment of aircraft performances.
Among all the altitudes, particular interest lies in the 10000 ft case (approximately 3000 m), which may be a typical cruise level, and in the 26000 ft case (nearly 8000 m), which may represent the limit for these aircraft (ceiling).
Compared to the Rotax 912 ULS/S, the 2S engine behaves in the same way as altitude increases. Figure 8a shows the variation of maximum power as a function of altitude, while figure 8b presents the same comparison in relative terms. The two graphs demonstrate the fundamental contribution provided by the support of the electric motor, in the hybrid power units. At 23000 ft, the hybrid system featuring a battery with a capacity of 2.4 kWh provides a power of 50 kW, versus the 30 kW of the Rotax engine, at take-off conditions. As take-off conditions generally have a short duration (less than 5 minutes), and the power delivered by the electric motor is about two thirds of its limit in continuous conditions, no particular problem is expected about the cooling of the electric system at high altitudes, even in presence of a significant reduction of the air density.
Figure 7 shows the operating points of the engine at full load in the supercharger map at 26000 ft: at ceiling, all the points fall in a region of high efficiency, at a safe distance from the surge line and the choke limit, even in the case of increasing the maximum engine speed from 4500 to 5500 rpm.

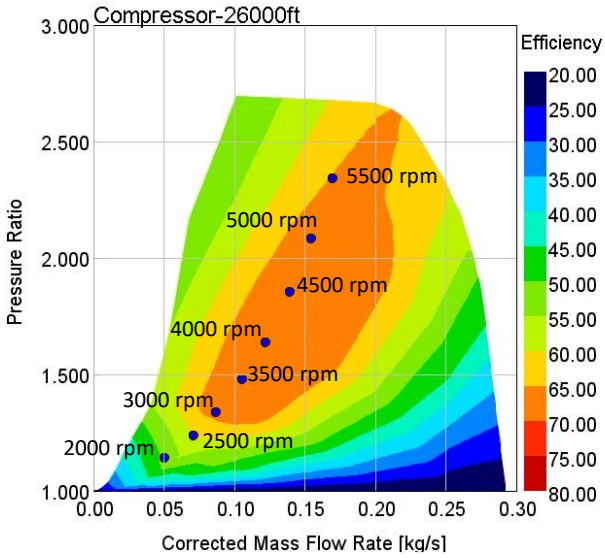

Figure 7. Compressor map with engine operating points at full load, at 26000 ft altitude

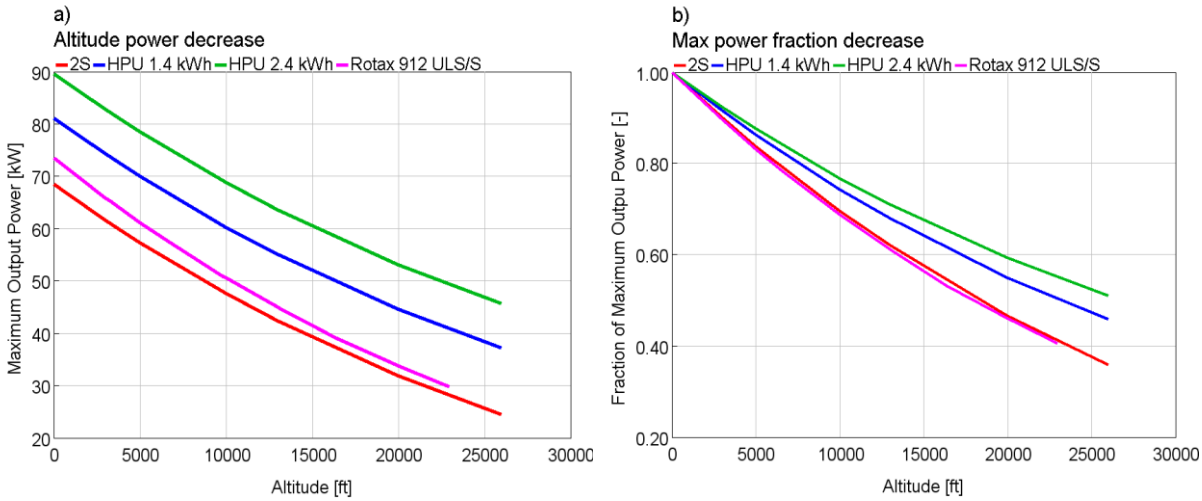

Figure 8a. Maximum Output Power vs altitude
Figure 8b. Fraction of maximum power vs altitude

Table 6 presents a summary about the main characteristics of all the types of power units analysed. In the two hybrid systems (HPU 1.4 kWh and HPU 2.4 kWh), the introduction of electrical components leads to a slight increase in total weight, compared to the Rotax engine (+2 and +7 kg, respectively); on the other hand, the performance has definitely improved: the peak power of the HPUs increases of 10 and 22%, respectively, while in continuous maximum power conditions the 2S engine alone is able to match almost perfectly the Rotax engine. In terms of thermo-mechanical loads, the 2S engine is equivalent or less stressed: while the mean piston speed at peak power is almost identical, the maximum BMEP is 27% lower.
In order to compare the different systems in terms of efficiency, a corrected Brake Thermal Efficiency (BTE*) is defined as follows:

$$BTE^* = \frac{P_{ice} + P_{EM}}{P_{fuel} + P_{batt}} \quad (2)$$

As visible in equation 2, BTE* takes into account not only the energy associated to the fuel consumed, but also the electrical energy taken from the battery. It is supposed that this energy is stored in the battery via an external charger, before take-off. As the product of the efficiencies of battery, inverter and electric motor is much higher than the BTE of the thermal engine, the higher is HL, the higher BTE*.
Under the hypotheses stated above, at peak power and at maximum continuous power, the HPUs are definitely more efficient than the Rotax: the maximum gain, at peak power, is +41%, resulting in a similar reduction of CO_2 (supposing the electric energy provided by renewable sources).
The authors acknowledge that these results are strongly related to the hypotheses made in the study: however, even in the worst scenario, when the battery is charged by the 2S engine, the efficiency of the HPUs remains higher than the Rotax. Unfortunately, no accurate figure can be given here, as the optimization of the charging strategy depends on the mission profile, and this aspect is beyond the scope of the current study.

Table 6. Main parameters of the analysed power units

Power unit	**Dry mass**	**Max continuous power**	**Peak power**	**Max BMEP**	**BTE* @ max continuous power**	**BTE* @ peak power**	**Mean piston speed @Peak Power**
	[kg]	**[kW@rpm]**	**[kW@rpm]**	**[bar]**	**[%]**	**[%]**	**[m/s]**
2S engine	39	68.4@4500	68.4@4500	8.65	35.7	35.7	11.9
HPU 1.4 kWh	62	78.3@4500(*)	81.1@4500(**)	8.65	38.3 (HL=0.19)	39.0 (HL=0.24)	11.9
HPU 2.4 kWh	67	84.9@4500(*)	89.6@4500(**)	8.65	39.9 (HL=0.25)	40.9 (HL=0.31)	11.9
Rotax 912 ULS/S	60	69@5500	73.5@5800	11.9	28.8 (HL=0)	29.0 (HL=0)	11.8

(*) Power available for 5 minutes (limit due to battery capacity).
(**) Power limited by the battery thermal resistance

Figure 9 shows the maximum power deliverable by the different systems as a function of the propeller speed (which is the same for all the cases). The graph reveals that the 2S engine requires the intervention of the electric motor only for propeller speeds higher than 2230 rpm. Moreover, HPU 2.4kWh is able to provide more power than the Rotax at any speed of the propeller.

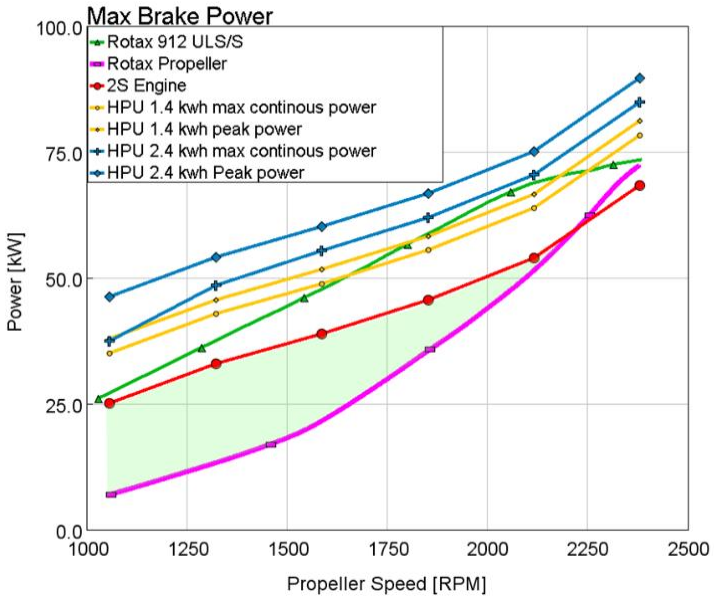

Figure 9. Full load power curves

At take-off condition, the HPU with a 1.4 kWh battery can deliver a power of 73.5 kW, equivalent to the Rotax maximum power, for a period of 10 min 24 s, more than two times the conventional interval of 5 minutes. Alternatively, the power unit would be able to deliver a higher power (+6.5%), for 5 minutes. This performance booster may be useful to reduce the climbing time.
Concerning the 2.4 kWh HPU version, it can deliver the same Rotax peak power (73.5 kW) for a duration of 17 min 24. Alternatively, the HPU would be able to provide 84.5 kW (+15,0 % respect to the Rotax engine) for 5 minutes.
Figure 9 shows in green the region where battery regeneration is possible. The difference between the 2S engine curve and the propeller resistance curve, multiplied by the efficiency of the electrical system, represents the instantaneous power available to recharge the battery under stationary operating conditions. Table 7 summarizes the results of the comparison among the analysed configurations.

Table 7. Summary of power unit performance

Power unit	Time range @ 73.5 kW	Max power for 5 min duration [kW]
Rotax 912 ULS/S	5 min	73.5
HPU 1.4 kWh	10 min 24 sec	78.3
HPU 2.4 kWh	17 min 24 sec	84.5

Figure 10 presents the trends of energy consumption as a function of the power required by the propeller, in steady conditions. The red and the blue curves represent the fuel consumption of the Rotax and of the 2S engine, respectively, while the green line shows the power adsorbed by the battery of the hybrid power unit. The graph confirms that fuel consumption is definitely reduced with the HPU, and that a small electrical assistance (≈7 kW) is needed only above 58 kW. Considering the typical power demand of an aircraft propeller (from 55% to 75% of the peak value, as reported on the Rotax manual), the consumption of electric energy for propulsion is zero, while the reduction of fuel consumption is 28%. This outcome means that is possible to increase by the same amount the operative range of the aircraft,

without any structural change (neglecting the effect of the additional 2 or 7 kg, associated to the hybrid power units, compared to the total weight of an ultralight aircraft, which is about 650 kg). Considering the same operative range, a significant increase of payload may be obtained by reducing the capacity of the fuel tank. As an example, considering the Falco EVO by Leonardo, equipped by the Rotax engine [13], the maximum payload is 100 kg; supposing a typical weight of the fuel tank equal to 110 kg, with a 28 % reduction of the mass of the stored fuel, it is possible to add about 30 kg of payload, without any change in the total weight and performance of the aircraft. A further weight saving derives from the possibility to use the compact battery of the hybrid system as a source of energy for the electrical equipment installed on the aircraft, avoiding the use of reinforced electric generators and heavy conventional batteries.

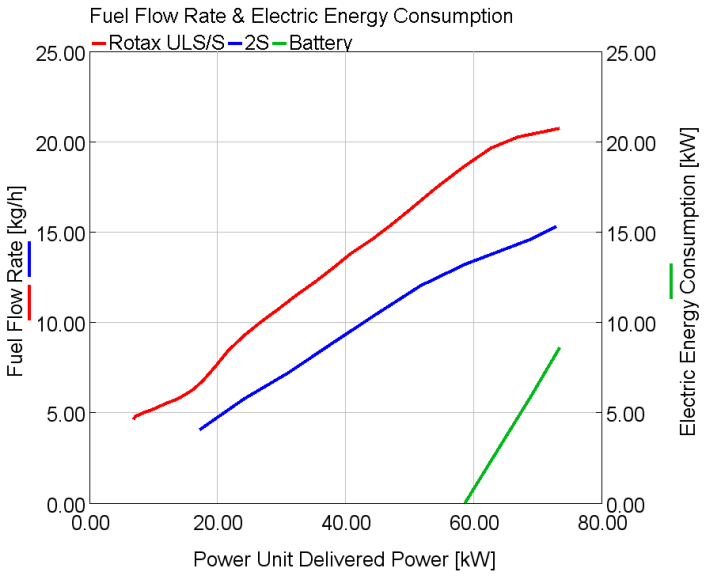

FIGURE 10. Fuel flow rate & electric energy consumption

Figure 11 finally shows CO2 emissions, calculated on the basis of fuel consumption (adopting the factors shown in Table 8), as a function of propeller power. The graph also evaluates the effects of the two battery charging strategies: electrical grid or thermal engine. This difference makes the HPU curves split over 58 kW, as the second strategy involves a higher number of energy passages (see Figure 12). Table 9 reports the efficiency factors used in the calculation. HPU CO2 emissions are up to 37 % lower than the Rotax engine, while the minimum gain is 16 %, This outcome was expected, and it is fully coherent with the results of the studies reported in [25]–[27].

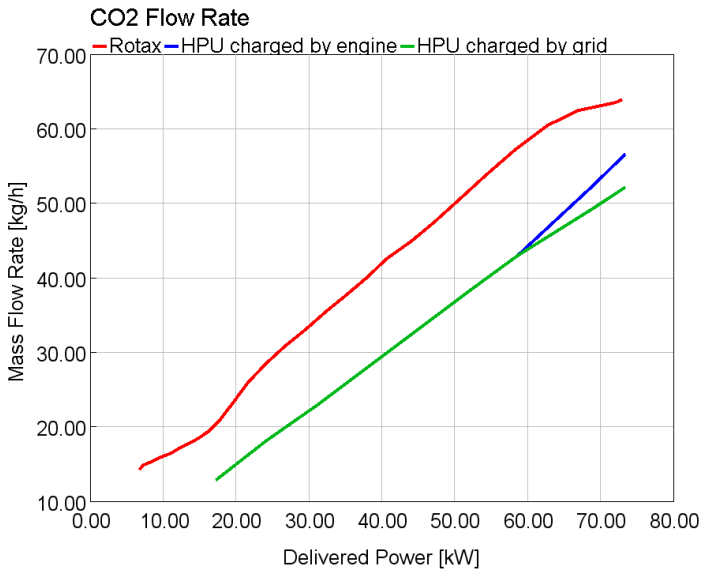

Figure 11. CO2 mass flow rate

Table 8. CO2 emission factors

Gasoline [28]	3.08 CO2_kg/Fuel_kg
Kerosene [28]	3.16 CO2_kg/Fuel_kg
Electricity [29]	0.48 CO2_kg/kWh

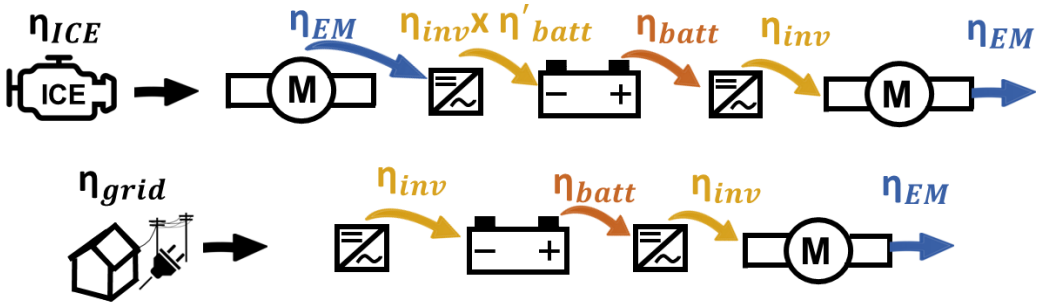

Figure 12. Energy chain for ICE recharging mode (up) and grid recharging mode (down)

Table 9. Efficiency factors

η_{ICE}	Depends on ICE operating point
η_{grid}	0.93
η_{EM}	0.90
η_{Batt}(*)	0.90 [30]
η'_{Batt}(**)	0.90 [30]
η_{inv}	0.95

(*)η_{Batt} is the battery efficiency during discharge
(**)η'_{Batt} is the battery efficiency during charge

CONCLUSIONS

The goal of the project described in this paper is to develop an innovative hybrid power unit for ultralight aircraft, able to replace, without modifications to the fuselage and with a minimum increase of weight, a conventional 4-S SI PFI gasoline engine, having a peak power of 73.5 kW. Reference is made to one the most widespread engine, the Rotax 912 ULS/S. However, differently from the Rotax engine, the new power unit must run on jet fuels.

The proposed engine has a boxer 4-cylinder design, like the Rotax, but its cycle is two-stroke, with piston controlled ports (no valves). The lubrication system is the same of the Rotax engine; air is pumped into the cylinders by means of a compact mechanical supercharger, without intercooler. The main novelty of the proposed engine consists in the combustion system, specifically developed with the support of CFD-3D simulations (not shown in the article, being at the moment a confidential subject).

The estimated weight of the new engine is 38.9 kg, more than 20 kg lighter than the Rotax, thanks to the lower number of components (no valves and camshafts, no liquid cooling system, no electric generator and starter and battery; the only additional parts are the supercharger and the high-pressure fuel pump). The estimation has been performed on a CAD model of the engine, integrated by measures on the commercial components (in particular the injection system, and the supercharger).

The weight saving provided by the 2-S engine has been exploited to add the electrical components of the hybrid system: electric motor, inverter, battery and wirings. Depending on the size of the battery, the total weight of the hybrid power unit exceeds by only 2 or 7 kg the weight of the Rotax 912 ULS/S engine, at the same conditions.

In terms of performance, according to the CFD-1D simulations carried out in this study, both HPUs are able to match the Rotax, and they can also increase the power output for a limited amount of time, depending on the battery capacity. For the smaller pack (1.4 kWh), a 6.5% of additional power is available for about 5 minutes, while for the bigger battery (2.4 kWh) an improvement of 15% may be obtained for the same amount of time.

However, the most important advantage related to the hybrid units is the strong reduction of fuel mass consumption, about 28% in typical cruise conditions. The improvement is related to the high efficiency of the thermodynamic cycle implemented in the 2-stroke CI engine, as well as to the lower mechanical losses (no valves).

A 28% reduction of fuel consumption can be translated into an equivalent increment of the operative range of the aircraft, or into an increase of payload (+30%, considering the Falco EVO aircraft).

Finally, compared to the Rotax engine, the hybrid power unit exhibits significantly lower CO2 emissions (from -12% to -37%), thanks to the improvement of fuel efficiency.

The authors acknowledge that the results presented in the paper may be affected by some uncertainties, due to the absence of experimental validation of the CFD models, that will be possible only after the construction of a physical prototype. However, it should be noted that, except for the combustion system, the design of the thermal engine is quite similar to previous projects of the authors, where the numerical models were calibrated with experimental data. As far as the electrical system is concerned, the uncertainty is limited by the use of well-known commercial components.

In conclusion, the proposed hybrid power unit appears as a promising solution to improve performance, efficiency, and sustainability of ultralight aircraft.

REFERENCES

[1] R. and M. ltd, ‘Global Ultralight Aircraft Market 2022-2026 - Research and Markets’. https://www.researchandmarkets.com/reports/5637150/global-ultralight-aircraft-market-2022-2026 (accessed May 08, 2023).

[2] ‘912 ULS / S’, *Rotax Aircraft Engines*. https://www.flyrotax.com/it/products/912-uls-s (accessed Jun. 09, 2023).

[3] ‘2200-Aero-Engine-Flyer-web-2-pages-20680-P12.pdf’. Accessed: Jun. 08, 2023. [Online]. Available: https://jabiru.net.au/wp-content/uploads/2023/02/2200-Aero-Engine-Flyer-web-2-pages-20680-P12.pdf

[4] ‘HKS Aviation Engines’. http://www.hksengines.com/ (accessed Jun. 08, 2023).

[5] ‘Groupe danielson’. http://www.danielson-eng.fr/en/danielson-100-td2-117.html (accessed Jun. 08, 2023).

[6] E. Mattarelli, C. A. Rinaldini, G. Cantore, and E. Agostinelli, ‘Comparison between 2 and 4-Stroke Engines for a 30 kW Range Extender’, *SAE Int. J. Alt. Power.*, vol. 4, no. 1, pp. 67–87, Nov. 2014, doi: 10.4271/2014-32-0114.

[7] R. Oswald, A. Ebner, and R. Kirchberger, ‘High Efficient 125- 250 cm ^{3} LPDI Two-Stroke Engines, a Cheap and Robust Alternative to Four-Stroke Solutions?’, presented at the Small Engine Technology Conference & Exposition, Sep. 2010, pp. 2010-32–0019. doi: 10.4271/2010-32-0019.

[8] E. Mattarelli, C. A. Rinaldini, and M. Wilksch, ‘2-Stroke High Speed Diesel Engines for Light Aircraft’, *SAE Int. J. Engines*, vol. 4, no. 2, pp. 2338–2360, Sep. 2011, doi: 10.4271/2011-24-0089.

[9] E. Mattarelli, F. Paltrinieri, F. Perini, C. A. Rinaldini, and M. Wilksch, ‘2-Stroke Diesel Engine for Light Aircraft: IDI vs. DI Combustion Systems’, presented at the SAE 2010 Powertrains Fuels & Lubricants Meeting, Oct. 2010, pp. 2010-01–2147. doi: 10.4271/2010-01-2147.

[10] S. Caprioli, C. Rinaldini, E. Mattarelli, T. Savioli, and F. Scrignoli, ‘Design of a Novel 2-Stroke SI Engine for Hybrid Light Aircraft’, presented at the SAE Powertrains, Fuels & Lubricants Digital Summit, Sep. 2021, pp. 2021-01–1179. doi: 10.4271/2021-01-1179.

[11] C. L. Bowman, J. L. Felder, and Ty. V. Marien, ‘Turbo- and Hybrid-Electrified Aircraft Propulsion Concepts for Commercial Transport’, in *2018 AIAA/IEEE Electric Aircraft Technologies Symposium (EATS)*, Jul. 2018, pp. 1–8.

[12] E. Frosina, C. Caputo, G. Marinaro, A. Senatore, C. Pascarella, and G. Di Lorenzo, ‘Modelling of a Hybrid-Electric Light Aircraft’, *Energy Procedia*, vol. 126, pp. 1155–1162, Sep. 2017, doi: 10.1016/j.egypro.2017.08.315.

[13] S. Fletcher, M.-C. Flynn, C. E. Jones, and P. J. Norman, ‘Hybrid electric aircraft : state of the art and key electrical system challenges’, *The Transportation Electrification eNewsletter*, vol. 2016, no. Sept, Art. no. Sept, Sep. 2016, Accessed: Jun. 11, 2023. [Online]. Available: http://tec.ieee.org/newsletter/september-2016/hybrid-electric-aircraft-state-of-the-art-and-key-electrical-system-challenges

[14] ‘falco-evo’. https://unmanned.leonardo.com/it/products/falco-evo (accessed Jun. 13, 2023).

[15] E. Chemali, M. Preindl, P. Malysz, and A. Emadi, ‘Electrochemical and Electrostatic Energy Storage and Management Systems for Electric Drive Vehicles: State-of-the-Art Review and Future Trends’, *IEEE Journal of Emerging and Selected Topics in Power Electronics*, vol. 4, no. 3, pp. 1117–1134, Sep. 2016, doi: 10.1109/JESTPE.2016.2566583.

[16] C. A. Rinaldini, S. Breda, S. Fontanesi, and T. Savioli, ‘Two-Stage Turbocharging for the Downsizing of SI V-Engines’, *Energy Procedia*, vol. 81, pp. 715–722, Dec. 2015, doi: 10.1016/j.egypro.2015.12.077.

[17] ‘Numerical optimization of supercharging and combustion on a two-stroke compression ignition aircraft engine’. https://journals.sagepub.com/doi/epub/10.1177/14680874221118174 (accessed May 27, 2023).
[18] C. A. Rinaldini, E. Mattarelli, and V. Golovitchev, ‘CFD Analyses on 2-Stroke High Speed Diesel Engines’, *SAE International Journal of Engines*, vol. 4, no. 2, pp. 2240–2256, 2011.
[19] E. Mattarelli, C. Rinaldini, and T. Savioli, *Port Design Criteria for 2-Stroke Loop Scavenged Engines*. 2016. doi: 10.4271/2016-01-0610.
[20] E. Mattarelli, C. Rinaldini, and P. Baldini, *Modeling and Experimental Investigation of a 2-Stroke GDI Engine for Range Extender Applications*, vol. 1. 2014. doi: 10.4271/2014-01-1672.
[21] E. Mattarelli, G. Cantore, C. A. Rinaldini, and T. Savioli, ‘Combustion System Development of an Opposed Piston 2-Stroke Diesel Engine’, *Energy Procedia*, vol. 126, pp. 1003–1010, Sep. 2017, doi: 10.1016/j.egypro.2017.08.268.
[22] F. Millo, A. Piano, B. Peiretti Paradisi, M. R. Marzano, A. Bianco, and F. C. Pesce, ‘Development and Assessment of an Integrated 1D-3D CFD Codes Coupling Methodology for Diesel Engine Combustion Simulation and Optimization’, *Energies*, vol. 13, no. 7, Art. no. 7, Jan. 2020, doi: 10.3390/en13071612.
[23] E. Mattarelli, S. Caprioli, C. A. Rinaldini, F. Scrignoli, D. Sparaco, and P. Caso, ‘Numerical optimization of supercharging and combustion on a two-stroke compression ignition aircraft engine’, *International Journal of Engine Research*, vol. 24, no. 6, pp. 2352–2368, Jun. 2023, doi: 10.1177/14680874221118174.
[24] A. Piano, F. Millo, F. Sapio, and F. C. Pesce, ‘Multi-Objective Optimization of Fuel Injection Pattern for a Light-Duty Diesel Engine through Numerical Simulation’, *SAE Int. J. Engines*, vol. 11, no. 6, pp. 1093–1107, Apr. 2018, doi: 10.4271/2018-01-1124.
[25] A. Warey, V. Gopalakrishnan, M. Potter, E. Mattarelli, and C. A. Rinaldini, ‘An Analytical Assessment of the CO_2 Emissions Benefit of Two-Stroke Diesel Engines’, presented at the SAE 2016 World Congress and Exhibition, Apr. 2016, pp. 2016-01–0659. doi: 10.4271/2016-01-0659.
[26] P. Tribotte *et al.*, ‘Two Strokes Diesel Engine - Promising Solution to Reduce CO2 Emissions’, *Procedia - Social and Behavioral Sciences*, vol. 48, pp. 2295–2314, 2012, doi: 10.1016/j.sbspro.2012.06.1202.
[27] C. Pirola, F. Galli, C. A. Rinaldini, F. Manenti, M. Milani, and L. Montorsi, ‘Effects of humidified enriched air on combustion and emissions of a diesel engine’, *Renewable Energy*, vol. 155, pp. 569–577, Aug. 2020, doi: 10.1016/j.renene.2020.03.155.
[28] J. B. Heywood, *Internal combustion engine fundamentals*, Second edition. New York: McGraw-Hill Education, 2018.
[29] ‘Efficiency and decarbonization indicators for total energy consumption and power sector. Comparison among Italy and the biggest European countries’, *ISPRA Istituto Superiore per la Protezione e la Ricerca Ambientale*. https://www.isprambiente.gov.it/it/pubblicazioni/rapporti/efficiency-and-decarbonization-indicators-for-total-energy-consumption-and-power-sector (accessed Jun. 29, 2023).
[30] T. B. Reddy and D. Linden, Eds., *Linden’s handbook of batteries*, 4th ed. New York: McGraw-Hill, 2011.